Biomechanical Changes After In Vivo Collagen Cross-Linking With Rose Bengal–Green Light and Riboflavin-UVA

Nandor Bekesi,[1] Patricia Gallego-Muñoz,[2] Lucía Ibarés-Frías,[2] Pablo Perez-Merino,[1] M. Carmen Martinez-Garcia,[2] Irene E. Kochevar,[3] and Susana Marcos[1]

[1]Instituto de Optica, Consejo Superior de Investigaciones Cientificas, Madrid, Spain
[2]Departamento de Biología Celular, Histología y Farmacología, GIR de Técnicas Ópticas para el Diagnóstico, Universidad de Valladolid, Valladolid, Spain
[3]Wellman Center for Photomedicine, Massachusetts General Hospital, Harvard Medical School, Boston, Massachusetts, United States

Correspondence: Nandor Bekesi, Instituto de Optica, Calle de Serrano 121, 28006 Madrid, Spain; nandorbekesi@gmail.com.

Submitted: January 12, 2017
Accepted: February 15, 2017

Citation: Bekesi N, Gallego-Muñoz P, Ibarés-Frías L, et al. Biomechanical changes after in vivo collagen cross-linking with rose bengal–green light and riboflavin-UVA. *Invest Ophthalmol Vis Sci*. 2017;58:1612–1620. DOI: 10.1167/iovs.17-21475

Purpose. To compare corneal biomechanical properties after in vivo and ex vivo cross-linking (CXL) using rose bengal–green light (RGX) or riboflavin-UVA (UVX).

Methods. Corneas of 30 rabbits were treated in vivo by the two CXL modalities monolaterally (Group 1) or bilaterally (Group 2). Rabbits in Group 1 were euthanized 1 month after treatments and in Group 2 two months after treatment. Ex vivo CXL was also performed. Eyes were measured by Scheimpflug air puff corneal deformation imaging (Corvis ST) under constant IOP. Corneal deformation parameters were assessed. Inherent corneal biomechanical properties were estimated using inverse finite element modeling.

Results. Peak to peak distance decreased 16% 2 months after RGX, and 4% and 20% 1 and 2 months after UVX, respectively. The equivalent Young's modulus (E_{eq}) increased relative to the control during the post treatment period for both RGX and UVX. The E_{eq} increased by factors of 3.4 (RGX) and 1.7 (UVX) 1 month and by factors of 10.7 (RGX) and 7.3 (UVX) 2 months after treatment. However, the E_{eq} values for ex vivo CXL were much greater than produced in vivo. The ex vivo E_{eq} was greater than the 1-month in vivo values by factors of 8.1 (RGX) and 9.1 (UVX) and compared with 2 month by factors of 2.5 (RGX) and 2.1 (UVX).

Conclusions. These results indicate that corneal stiffness increases after CXL, and further increases as a function of time after both RGX and UVX. Also, while biomechanical properties determined after ex vivo CXL are indicative of corneal stiffening, they may not provide entirely accurate information about the responses to CXL in vivo.

Keywords: corneal biomechanics, cross-linking, inverse modeling, computational modeling

Corneal shape, and therefore optical function, is compromised in certain diseases that mechanically weaken corneal structure (e.g., keratoconus) or by iatrogenic ectasia after certain corneal refractive procedures. Corneal cross-linking (CXL) is generally accepted and frequently used clinically to treat keratoconus and also to strengthen the cornea after LASIK.[1] In conventional CXL (the so-called Dresden protocol), the cornea is de-epithelized, instilled with the photo-initiator 0.1% riboflavin (RF) in 20% dextran solution intermittently for 30 minutes, then irradiated with UVA light (366 nm, 3 mW/cm^2) for 30 minutes. Alternative CXL procedures using UVA (UVX) have been developed in order to decrease the treatment time by increasing the light irradiance,[2,3] to avoid the de-epithelialization (epi-off treatment), or to avoid corneal thinning by using hypo-osmolar RF solutions.[4,5] However, in this study, we studied the effects of the conventional Dresden protocol, which complies to the method approved by the Food and Drug Admiration and was followed in previous studies on UVX in rabbits.[6–10]

Recently another CXL method has been proposed that uses rose bengal (RB) as the photosensitizer and green light (532 nm) and is termed RGX.[11,12] The photochemical process initiated by RGX had previously been used to create covalent bonds between collagen molecules on two different surfaces for attaching a bandage to the corneal surface,[13] to sealing skin wounds,[14] and photobonding an intraocular lens to the interior of the lens capsule.[15] The effect of RGX on the corneal biomechanics has been demonstrated by strip extensiometry,[11,12] by Brillouin microscopy[16] and in whole-eye globes by air puff deformation measurements and inverse mechanical modeling.[6] The corneal stiffening produced by RGX occurs closer to the anterior surface than stiffening by UVX because penetration of RB into the stroma is limited by its strong association with collagen. Within the cross-linked regions, RGX decreased elasticity to a greater extent than UVX in an ex vivo study.[6]

The efficacy of CXL for stiffening the cornea has been demonstrated in most cases by biomechanical testing using techniques such as uniaxial tensiometry on corneal strips, which is necessarily restricted to ex vivo measurements.[10,17–19] On the other hand, clinical attempts to measure corneal mechanical properties are still subject to validation and cannot yet be used to evaluate CXL-induced changes in cornea stiffness. Air-puff deformation imaging is a promising technique to obtain corneal mechanical properties in vivo, although these systems are still marketed as clinical tonometers. One of the

most well-known types is the Ocular Response Analyzer (ORA; Reichert, Inc., Depew, NY, USA), which uses an electro-optical collimation detector to monitor the deformation of the cornea due to an air pulse.[20] Besides the IOP, ORA provides some biomechanics-related values (e.g., corneal resistance factor); however, its relation to Young's modulus or any other mechanical measures remains unknown. Air-puff optical coherence tomography (OCT)[7] and Corvis ST (Oculus, Wetzlar, Germany)[6,21] use a controlled air puff and spectral OCT imaging or an ultra-high speed Scheimpflug camera, respectively, to capture the corneal dynamic deformation. We have recently shown that it is possible to reconstruct corneal inherent mechanical parameters from corneal deformation imaging using inverse optimization.[6] In a recent study, Bekesi et al.[22] demonstrated the validation of this technique on hydrogel model corneas and porcine corneas. Inherent material parameters were reconstructed from air puff deformation imaging and inverse optimization modeling that matched those obtained on the same samples using uniaxial extensiometry.

Clinical studies evaluating the effect of CXL on keratoconic patients using air-puff techniques offer conflicting conclusions on the effect of CXL on the measured parameters. Greenstein et al.[23] found no significant improvement in biomechanics 1 year after CXL using ORA. De Bernardo et al.[24] measured 57 eyes by ORA before and during a 24 month follow-up after CXL. However, results showed no significant changes in the so-called corneal hysteresis and corneal resistance factor deformation parameters. It is likely that these controversial results arise from the dependence of the corneal deformation parameters on other factors, such as IOP, corneal thickness, and corneal shape. Thus, there is a real need for estimating the material properties of cornea in isolation.

Many ex vivo experimental studies have demonstrated an increase in corneal stiffness following both UVX and RGX on rabbit, porcine, bovine, and human corneas.[11,18,19,25] We have recently reported[6] corneal mechanical properties (elasticity constants and time constants, as well as an equivalent Young's modulus) in rabbit corneas treated with UVX and RGX obtained from applying our inverse optimization method[26] to air-puff corneal deformation imaging data. In this and most previous studies, the treatments were performed ex vivo and measurements of the corneal mechanical properties were assessed immediately after treatment. However, hydration is of utmost importance in corneal biomechanical tests. In standard CXL the modulation of hydration produced by the hypo-osmolar RF solution may interfere on the outcomes of mechanical measurements, as those have been shown to depend on hydration.[27] For example, several studies have found that the observed structural changes (fibril diameter and interfibrillar spacing) after immediate CXL of postmortem human corneas were more likely a consequence of treatment-induced changes in tissue hydration rather than cross-linking.[28] Some results are available from evaluation of corneal microstructure and histology in corneas following CXL in vivo in experimental models (usually rabbits). In this study, we measured the biomechanical changes 1 and 2 months after the treatments, ensuring that both the temporary dehydration during the treatment and the postmortem hydration are ruled out.

However, corneal mechanical measurements following in vivo CXL, which represent a more realistic clinical situation, are uncommon. Kling et al.[9] used two-dimensional flap extensiometry to assess corneal deformation of corneal flaps (of different depths) to increased IOP, 1-month after UVX in rabbits. Zhu et al.[12] used uniaxial tensiometry to measure stiffness and Young modulus 1 and 28 days after RGX in rabbits.

This study was designed to compare the effects of in vivo versus ex vivo CXL on biomechanical properties using a noninvasive imaging technique, air-puff Scheimpflug corneal deformation imaging and inverse modeling to estimate the inherent corneal mechanical properties. Two CXL modalities, namely UVX and RGX, were used for this evaluation because of the differences in the spatial distribution of the crosslinks. Eyes treated in vivo were examined 1 and 2 months post surgery and the results compared with ex vivo–treated eyes.

Methods

Samples

Thirty New Zealand rabbits were used. The rabbits received unilateral or bilateral CXL treatments in vivo. Seventeen rabbits (Group 1) received unilateral CXL treatments (8 RGX and 9 UVX) with the contralateral eye as a control and were euthanized 1 month after the treatments. Thirteen rabbits (Group 2) received bilateral RGX and UVX treatments and were euthanized 2 months after CXL. Ten of the control eyes of the rabbits in Group 1 were used as a further control and received ex vivo treatments (same modality as the contralateral in vivo–treated eye) after the measurements. Results of the clinical analysis are presented in a recent study by Gallego-Muñoz et al. (manuscript submitted, 2017).

The Animal Ethics Committee of the University of Valladolid, Spain approved all protocols. Animals were cared for and handled according to the guidelines of the ARVO Statement for the Use of Animals in Ophthalmic and Vision Research.

CXL Procedures

Rabbits were anesthetized with a single intramuscular injection of 50 mg/kg of ketamine (Imalgene 1000; Meruak, Lyon, France), plus 7 mg/kg of Xilacine (Rompun; Bayer, Leverkusen, Germany), followed by topical application of 0.5% tetracaine hydrochloride and 1 mg of oxybuprocaine (Colircusi Anestésico Doble; Alconcusí SA, Barcelona, Spain). After de-epithelialization in the central 8-mm diameter area the corneas were either left untreated for controls or treated by one of the following treatments.

Rose Bengal – Green Light Cross-Linking (RGX). The RB solution consisted of 0.1% RB in PBS. Green light CXL was performed using a custom-developed light source, which incorporated a 532-nm laser with an output irradiance of 0.25 W/cm^2 (MGL-FN-532; Changchun New Industries, Changchun, China) with a collimating lens that provided an 11-mm Gaussian profile beam at the sample plane. The RGX protocol was: (1) 2-minute staining with RB, then irradiation for 200 seconds, and (2) 30-second staining with RB, then green light irradiation again for 200 seconds (total fluence, 100 J/cm^2).

Riboflavin – UVA Light Cross-Linking (UVX). The RF solution consisted of 0.125% riboflavin-5-phosphate in 20% Dextran T500 (Farmacia Magistral, Madrid, Spain). Ultraviolet A cross-linking was performed using an IROC UVA lamp (370 nm, 3 mW/cm^2; Institute for Refractive and Ophthalmic Surgery, Zurich, Switzerland). The UVX protocol was: (1) 30-minute staining with RF, with one drop applied every 5 minutes, and (2) UVA irradiation for 30 minutes, with one drop of RF applied every 5 minutes.

Untreated contralateral eyes of Group 1 were treated less than 24 hours after enucleation following same treatment UVX and RGX protocols used for the in vivo treatments in the contraleral eye. The eyes were measured by Corvis ST before and after CXL without removing them from the holder.

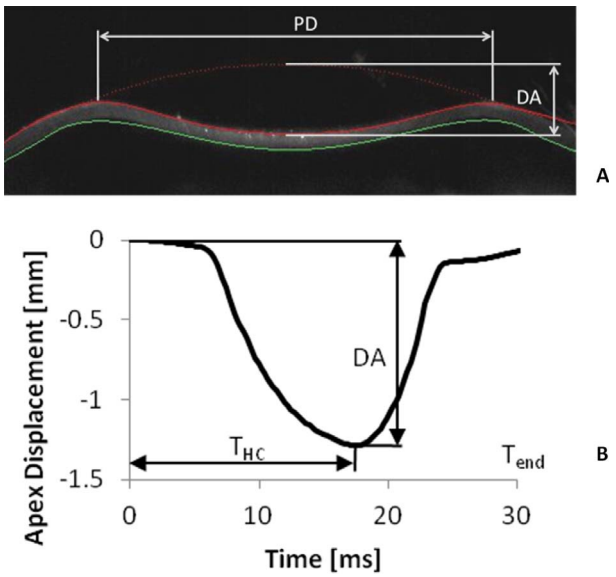

FIGURE 1. Corvis ST image of a cornea at highest concavity (**A**) and the temporal profile (**B**).

Air Puff Deformation Imaging

Eyes were excised and mounted immediately (<5 minutes) in a custom-made eye holder consisting of two movable semicircular parts that allowed holding the eye along its equator. After mounting the eye in the holder, a needle was inserted through the optic nerve head to control IOP, which was kept constant at 15 mm Hg by a water column system. Air puff corneal deformation measurements were taken using a Scheimpflug-based imaging system.

Air Puff System. A commercial system was used (Corvis ST) that combines air puff with high-speed Scheimpflug imaging. The Corvis ST system has an air compressor emitting a quick, controlled air puff (~20 ms). The release of the air puff is synchronized with an ultra-high speed Scheimpflug camera that captures 140 horizontal cross-sectional corneal images during the approximately 30-ms deformation event (i.e., at a rate of approximately 4330 images/sec) with a resolution of 640×480 pixels. The eye is positioned in front of the system at a distance of 11 mm between the apex and the air tube. Upon air puff stimulation, the cornea becomes concave around the apex and then returns to the initial shape in 30 ms.

Result Parameters. The corneal apex displacement as a function of time (temporal corneal deformation) and the cross-section of deformed shape of the cornea at maximum concavity (spatial corneal deformation) were analyzed. The following parameters were retrieved (Fig. 1): (1) maximum deformation amplitude (DA), which is the displacement of the corneal apex at maximum deformation; (2) peak-to-peak distance (PD), which is the lateral distance between the two peaks in the corneal profile at maximum deformation; (3) central corneal thickness (CCT), which is the thickness of the cornea at the apex; (4) time of highest concavity (T_{HC}), which is the time of the maximum corneal deformation; and (5) temporal symmetry factor (*TS*), which is the ratio of the two areas under the apex displacement versus time curve separated by the T_{HC}, and can be calculated from Equation 1:

$$TS = \frac{\sum_{T_0}^{T_{HC}} \Delta Y_{\text{apex}}(t)}{\sum_{T_{HC}}^{T_{\text{end}}} \Delta Y_{\text{apex}}(t)} \quad (1)$$

where T_0 is the starting time of the air puff, T_{end} is the ending time of the deformation event, and $\Delta Y_{\text{apex}}(t)$ is the displacement of the apex at a given time.

Statistical Analysis

Statistical analysis was carried out on the result parameters using 1-way ANOVA in Microsoft Office Excel (v2007; Redmond, WA, USA). The parameters of the different groups were compared with the control results. The significance level was set at P less than 0.05.

Numerical Simulations

Inverse mechanical modeling was performed incorporating finite element (FE) simulations in order to obtain and compare the mechanical properties of the control and the CXL corneas. The fundamentals of the inverse modeling approach is described in detail by Kling et al.[26] Uniaxial tensile tests were modeled by FE using the inherent material properties from the inverse modeling, and the stress-strain relations were plotted with the aim of comparing the material characteristics.

Inverse Modeling. The inverse modeling process consisted of running a (1) FE simulation of the air-puff test on the eye globe, (2) comparing the spatial and temporal profiles by calculating the sum of the squared differences of the measured and simulated curves, and then (3) changing the material parameters in the model and restarting the cycle.

Finite Element Models. A finite element model of the rabbit cornea was built assuming axial symmetry. Corneal thickness was modeled from the corresponding average experimental data (from the Corvis ST measurements) shown in Table 1.

Rose bengal–green light and UVX have been reported to stiffen the stroma in a different depth. Cherfan et al.[11] reported that RGX affects the top 100 μm of the corneal stroma. Although, the ex vivo thickness of the RGX cornea (RGX0) was relatively high (429 μm), the anterior cross-linked part was also assumed to be 100 μm, as this has consistently found to be the penetration depth of the RB photo-initiator in corneas.[16] Riboflavin-UVA has been shown to affect 300 μm of the human cornea[29] and approximately 400 μm of the porcine cornea. A recent study[8] suggests that the UVX-treated to total stromal thickness ratio of two-thirds is valid in rabbits. The control corneas were assumed to have uniform mechanical properties along its thickness, while the CXL corneas were modeled with two different material models in the anterior and the posterior part; the CXL anterior part was 100 and 143 to 188 μm for RGX and UVX, respectively, similarly to the models in Reference 6 (Table 1).

Material Models. The corneal material was modeled by a nonlinear, hyperelastic Mooney-Rivlin (MR) material model with five parameters along with a Prony-series visco-elastic model. The strain energy density function (*W*) for an

TABLE 1. Thickness Parameters for the Finite Element Models of Different Conditions

Thickness Parameter	Control	RGX 1	RGX 2	UVX 1	UVX 2	Virgin, RGX	RGX 0	Virgin, UVX	UVX 0
Total CCT, μm	316	245	244	269	282	441	429	479	215
Thickness of CXL layer, μm	–	100	100	179	188	–	100	–	143

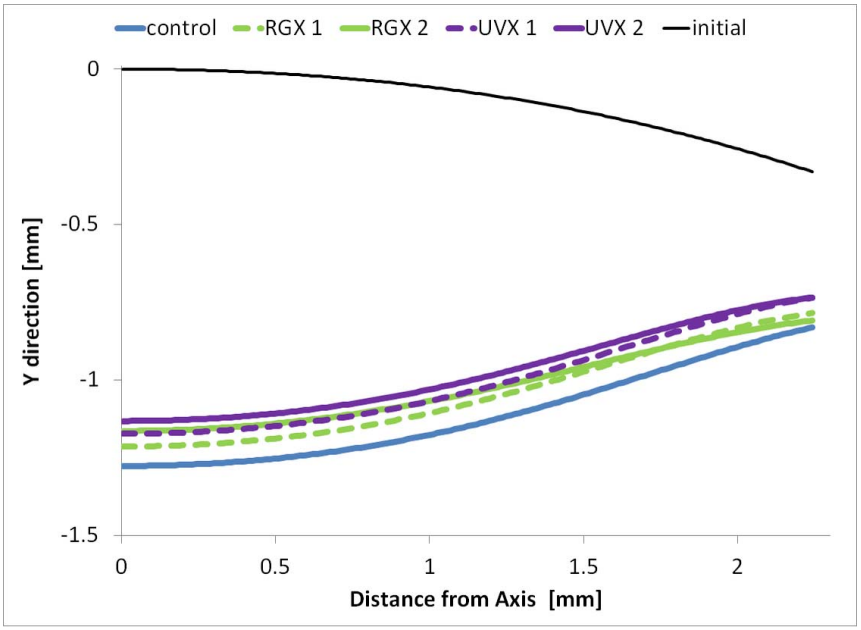

FIGURE 2. Spatial corneal deformation profiles of control, RGX, and UVX corneas, 1 and 2 months after CXL.

incompressible Mooney-Rivlin material is Equation 2:

$$W = C_{10}(\bar{I}_1 - 3) + C_{01}(\bar{I}_2 - 3) + C_{20}(\bar{I}_1 - 3)^2 + C_{11}(\bar{I}_1 - 3)(\bar{I}_2 - 3) + C_{02}(\bar{I}_2 - 3)^2 \quad (2)$$

where $\bar{I}_1$ and $\bar{I}_2$ are the first and the second invariant of the left Cauchy–Green deformation tensor; C_{10}, C_{01}, C_{20}, C_{11}, C_{02} are material parameters. The limbus and the sclera were modeled as isotropic elastic materials with Young's moduli $E_{\text{limbus}} = 1.76$ MPa and $E_{\text{sclera}} = 3.52$ MPa, respectively.

The pressure from the air puff was modeled as a pressure load on the top of the surface elements of the cornea as a function of location and time (as described by Kling et al.[26]). The interior of the eye was modeled with incompressible fluid elements, which have an extra degree of freedom for pressure.[30] A pressure of 15 mm Hg was applied on these elements as initial condition to model the IOP. The nodes along the equator were fixed, modeling the grip of the eye holder.

Optimization Process

D in Equation 3 was minimized, where D_{sp} and D_t are the sum of squared differences between measured and simulated spatial and temporal profiles, respectively (see Equations 4 and 5).

$$D = D_{sp} + D_t \quad (3)$$

$$D_{sp} = \sum_{i=0}^{X_{\text{end}}} (y_{\text{meas},i} - y_{\text{sim},i})^2 \quad (4)$$

$$D_t = \sum_{j=0}^{T_{end}} (y_{\text{meas},j} - y_{\text{sim},j})^2 \quad (5)$$

A two-step optimization algorithm was used. The first step was a global optimization using brute force screening with relatively large steps to find the global minimum. The second step used the result of the first step as a starting point for the local adaptive optimization. This step used a downhill simplex algorithm. The five Mooney-Rivlin material parameters (Equation 2) and relative modulus (RM)1 and RM2 relative moduli of the viscoelastic model were the design variables of the optimization in the inverse modeling process.

The reconstructed material models represented by plotting their stress–strain curves. The equivalent Young's modulus (E_{eq}) is calculated as the secant modulus at a strain of 0.1.

RESULTS

Measured Spatial and Temporal Profiles: In Vivo Treatments

Rose bengal–green light and UVX treatments changed the corneal deformation in response to air-puff perturbation. Figure 2 shows the average spatial profiles of the control and CXL eyes, 1 and 2 months after treatments. The average SDs in these curves were 0.12 mm for control eyes, and 0.1 mm for RGX, and 0.08 mm for UVX (average 1–2 months). Rose bengal–green light and UVX corneas in the 1-month group deformed less than the control, as expected based on our previous ex vivo treatment study.[6] The 2-month results show an even more pronounced decrease in the entire spatial deformation (Fig. 2) and a slower deformation during the initial part of the deformation event followed by a faster recovery (Fig. 3). This occurs similarly in both RGX and UVX.

Corneal Deformation Parameters: In Vivo Treatments

Figure 4 shows the average corneal deformation parameters. Compared with the control group, RGX and UVX appeared to decrease DA by 5% to 11%, although these changes were not statistically significant (Fig. 4A). However, RGX and UVX produced significant changes in PD, CCT, and T_{HC} values. Peak-to-peak values decreased in all groups: RGX decreased PD slightly after 1 month and by 16.4% after 2 months and UVX produced a decrease in PD of 4% after 1 month and 20% after 2 months (Fig. 4B). Similarly, RGX decreased CCT by 23% after both 1 and 2 months and UVX decreased CCT by 15% after 1 month and by 11% after 2 months (Fig. 4C). In addition, RGX

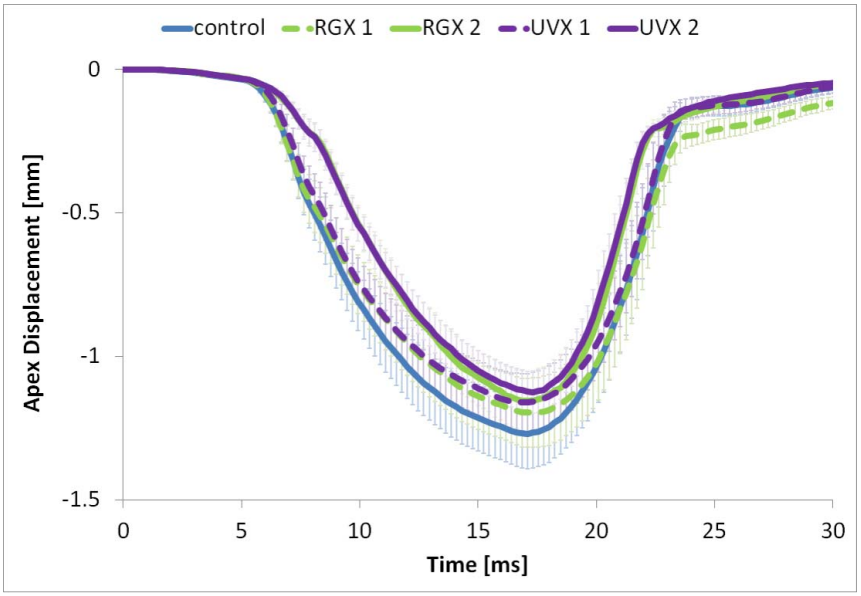

Figure 3. Temporal profiles of control, RGX, and UVX corneas, 1 and 2 months after CXL.

increased T_{HC} by 2.7% after 1 month and by 0.49% after 2 months (Fig. 4D) and UVX increased T_{HC} by 1.6% after 1 month (although not statistically different) and by 1.45% after 2 months (Fig. 4E). Neither RGX nor UVX changed TS in a statistically significant way (Fig. 4E).

Corneal Deformation Parameters: Ex Vivo Treatments

Figure 5 compares corneal deformation parameters obtained in eyes immediately after ex vivo application of CXL (UVX0 and RGX0), which were contralateral eyes of those that received in vivo CXL) and in eyes after in vivo CXL at two time-points after CXL (1 month labeled UVX1, RGX1 and 2 months labeled UVX2, RGX2). The in vivo corneal deformation parameters were normalized by dividing the CXL data by the control data, while ex vivo results were normalized by the results measured in the same eyes before treatment. Thus, we were able to compare the effects of CXL immediately with those observed 1 and 2 months after treatments. Error bars show the normalized SD.

Compared with pretreatment values ex vivo CXL produced the following changes: DA was 20% lower for UVX0 and 13% for RGX0; PD was 7% lower for UVX0 and 6% for RGX0; CTT was 65% lower for UVX0 and 2% lower for RGX0; TS 28% lower for UVX0, 13% for RGX0.

Several differences in responses to ex vivo versus in vivo treatments are apparent in Figure 5. This is most noticeable in the measured CCT values that show a thinner cornea after UVX0 than after in vivo treatment (1 and 2 months). Interestingly, the opposite was found for RGX, namely, thinner corneas after 1 and 2 months than for ex vivo treatment. Differences were also found between UVX0 and 1 and/or 2 month post in vivo UVX treatment for DA, PD, T_{hc}, and TS. For RGX, differences were found between RGX0 and in vivo groups for DA and PD.

FE Simulations

Reconstructed Material Properties. The reconstructed material parameters of the control and in vivo CXL corneas as well as the ex vivo results are summarized in Table 2. The material properties can be assessed better by comparing the mechanical response of the materials to certain loads; it is traditionally performed by plotting the stress–strain relations (Fig. 6). The stress is the applied mechanical force over the cross-section area, while the strain is the deformation divided by the original length of the sample.

Corneal Biomechanical Properties: Time From Treatment. All corneas were stiffer at 2 months rather than 1 month after CXL, for both RGX and UVX. Corneal cross-linking corneas were stiffer than control corneas in all cases. Rose bengal–green light produced an increase of the equivalent modulus of elasticity (E_{eq}) by factors of 3.4 and 10.7, at 1 and 2 months after treatment, respectively. Riboflavin-UVA produced an increase in E_{eq} by factors of 2.4 and 10.3 at 1 and 2 months after treatment, respectively.

Corneal Biomechanical Properties: RGX Versus UVX. The equivalent elasticity in the CXL-treated region was two times higher for RGX than UVX 1 month after treatment and 1.45 times higher after 2 months for in vivo treatments, and 1.8 times higher for ex vivo treatments.

Corneal Biomechanical Properties: In Vivo Versus Ex Vivo CXL. Ex vivo treatments showed a larger corneal stiffening effect for both CXL modalities by factors of 2.5 for RGX and 2.1 for UVX comparing ex vivo CXL and 2 month post in vivo CXL. The difference in viscoelastic relative modulus of RGX 2 months after in vivo and ex vivo CXL was less than 1%, while for UVX it differed by a factor of 15.

Discussion

Measuring air-puff corneal deformation and estimating biomechanical properties of the corneas from finite element modeling revealed that in vivo CXL treatments increased cornea stiffness for both RGX and UVX. However, the magnitude of the increase was significantly less than for ex vivo CXL treatments suggesting that results of CXL efficacy based solely on ex vivo treatments should be interpreted with caution. The changes in deformation parameters produced by RGX versus UVX were similar, but not entirely the same. In addition, determining the air puff deformation parameters at 1

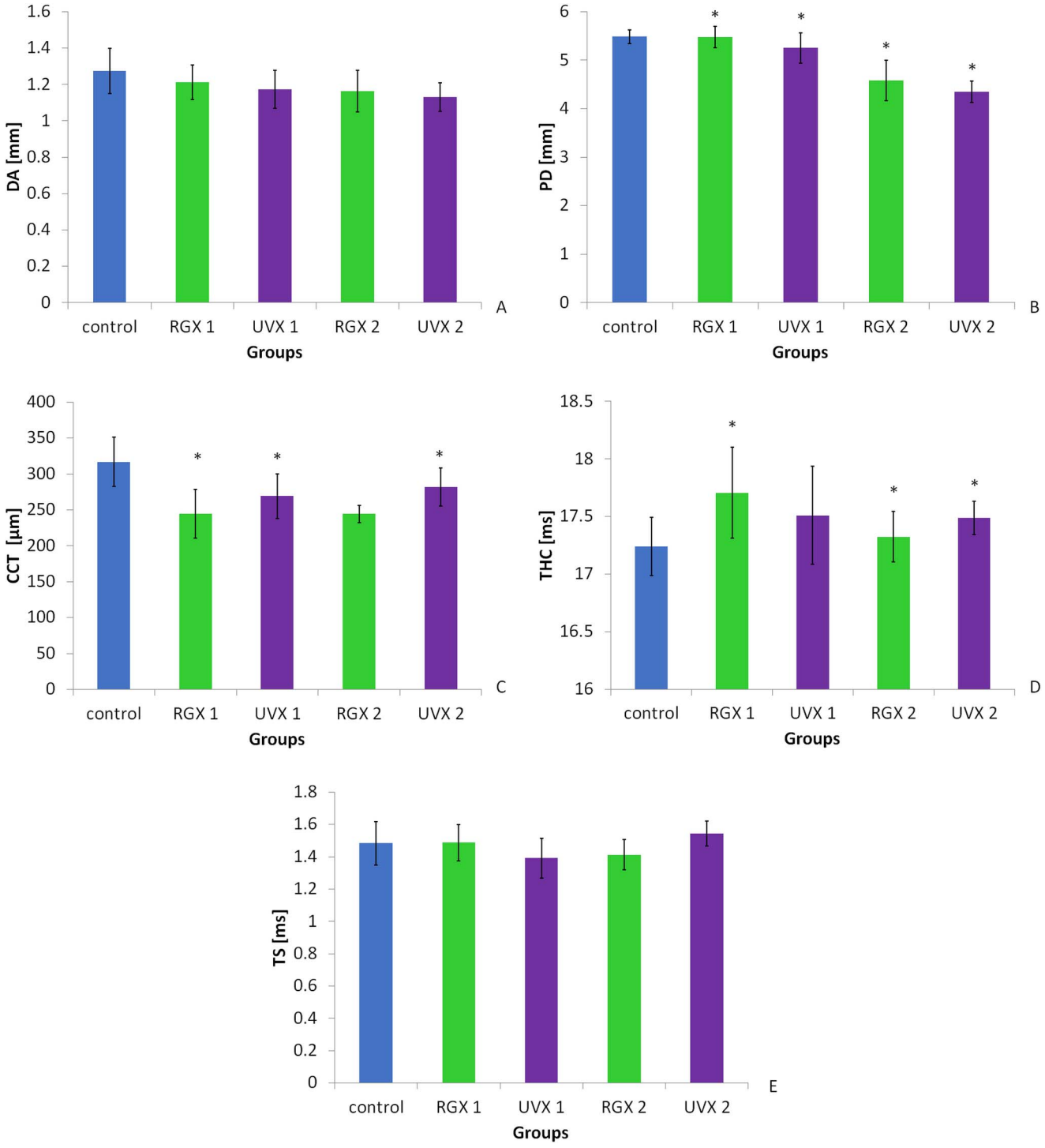

FIGURE 4. Average corneal deformation parameters of control, RGX, and UVX corneas measured 1 (RGX 1 and UVX 1) and 2 months (RGX 2 and UVX 2) after treatments. *Error bars* represent the SD. *$P < 0.05$ between control and CXL eyes.

and 2 months post treatment demonstrated that the cornea stiffness increased over this period and may reflect the remodeling process.

Previous ex vivo CXL treatments and immediate measurements have demonstrated increased stiffness, however, the treatment conditions were far from a real clinical situation. Examples include studies showing increased corneal stiffness following standard UVX by factors of 1.6, 2.0, and 1.2 in porcine, rabbit, and mouse eyes, respectively.[18,19,31] An ex vivo study of RGX also reported increased cornea stiffness, up to 4.4-fold in rabbit eyes.[11] And in an previous ex vivo study, we found 10- and 6-fold increases in Young's modulus in the cross-linked region after RGX and UVX, respectively, using finite element modeling from air-puff corneal deformation.[6] In the current study, identical CXL treatments were carried out ex vivo and in vivo and the same measurement techniques were used by the same investigators thus allowing an accurate comparison of cornea responses to in vivo versus ex vivo CXL.

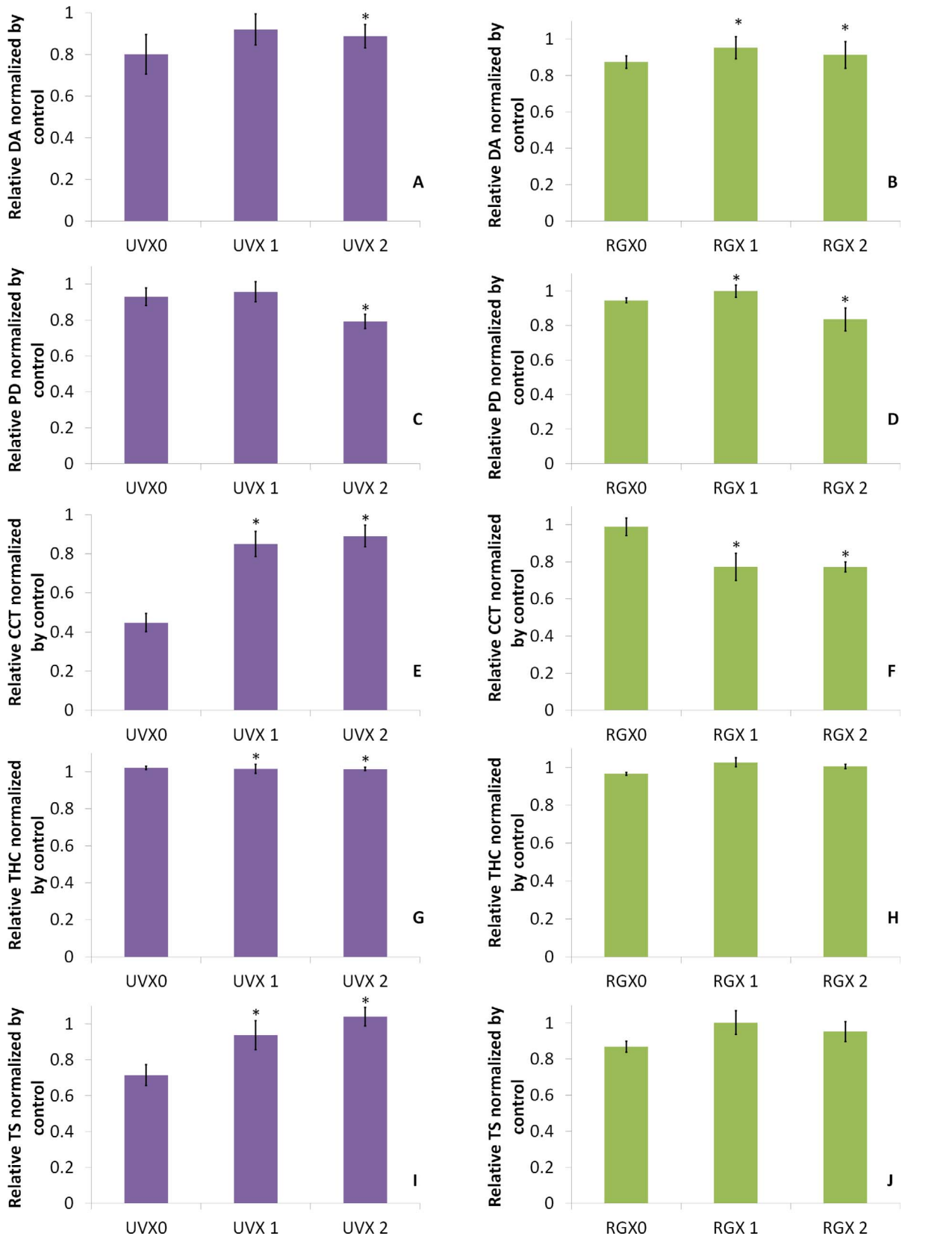

Figure 5. Relative corneal deformation parameters of ex vivo (RGX0 and UVX0) and in vivo cross-linked corneas measured 1 (RGX 1 and UVX 1) and 2 months (RGX 2 and UVX 2) after treatments. The ex vivo deformation parameters were normalized by the results of the same eye before treatment, and the in vivo parameters were normalized by the control data. *Error bars* represent the SD. $^*P < 0.05$ between ex vivo and in vivo CXL corneas.

Table 2. Reconstructed Material Parameters of Control and In Vivo and Ex Vivo CXL Corneas

Material Parameter	Control	RGX 1	UVX 1	RGX 2	UVX 2	RGX0	UVX0
C_{10}, MPa	0.079	0.19	0.112	0.336	0.11	0.470	0.345
C_{01}, MPa	0.069	0.166	0.0984	0.293	0.0967	0.403	0.301
C_{20}, MPa	10.51	77.21	50.49	218.01	96.95	56.04	39.929
C_{11}, MPa	0.009	0.0661	0.0432	0.186	0.083	0.051	0.0341
C_{02}, MPa	3.94	28.96	18.94	81.78	36.37	21.02	14.98
RM1	0.712	0.62	0.597	0.781	0.618	0.78	0.0466
RM2	0.103	0.0897	0.0863	0.113	0.0895	0.13	0.00674
E_{eq}, MPa	1.41	4.73	2.37	15.06	10.33	38.35	21.7

Corneal deformation parameters, which are descriptive of some of the viscoelastic responses, differed between in vivo and ex vivo CXL treatments with generally greater changes observed after ex vivo CXL. Decreases in DA and PD are consistent with increased stiffness of the cornea. A trend toward a decrease in DA was found for in vivo CXL although a significant decrease was only observed for ex vivo CXL. In contrast, the decrease in PD was greater for in vivo (4%–20%) than for ex vivo CXL (6%–7%). Time-dependent parameters (T_{HC} and TS) were most affected after ex vivo CXL. For UVX, these differences in viscoelastic-related parameters between in vivo and ex vivo treatments may be related to corneal hydration. Central corneal thickness can be taken as a good marker for corneal hydration. Central corneal thickness decreased substantially (65%) after ex vivo UVX due to the dehydrating effect of dextran in the RF solution and returned to within 15% and 11% of controls at 1 and 2 months. For RGX, CCT did not change after ex vivo treatment but showed a 23% decrease at 1 and 2 months.

The material properties of cornea derived from finite element modeling reflect these differences in deformation parameters between ex vivo and in vivo CXL treatments. The ex vivo–treated corneas showed greater equivalent Young's moduli (E_{eq}) than those treated in vivo with CXL by factors of 2.35 and 2.11 for RGX and UVX at 2 months, respectively.

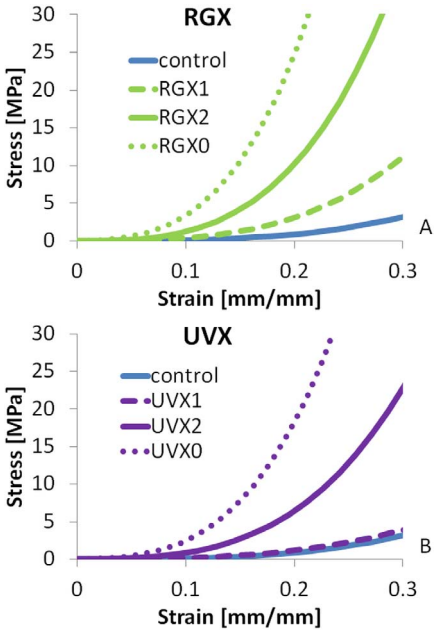

Figure 6. Stress–strain curves of the reconstructed materials of (**A**) RGX and (**B**) UVX. *Dotted lines* represent ex vivo CXL corneas measured immediately after treatment (RGX0 and UVX0).

Taken together, the results of air-puff deformation and the calculated material properties of cross-linked cornea indicate that although both in vivo and ex vivo CXL stiffen the cornea, the magnitudes of the changes differ and suggest that biomechanical properties measured after ex vivo CXL may not be adequate for preclinical evaluations of CXL techniques.

The in vivo CXL-treated corneas showed increased stiffness in the treated region with increasing time post surgery; the 1 to 2 month increase in E_{eq} was 3.18 for RGX and 4.36 for UVX (Table 2). These values are similar, although somewhat larger than, a previously reported increase in Young's modulus measured by uniaxial tensiometry 2 and 28 days after RGX.[12] Because the chemical cross-links produced by CXL that increase stiffness are produced at the time of treatment, these observed changes are likely to be associated with corneal remodeling and natural age-related changes in the cornea.[32] These changes are consistent with clinical reports of improvement in visual acuity and also elongation of the eyes during months following UVX, which may also result from corneal remodeling during healing.[33,34]

The cornea deformation parameters measured after RGX or UVX in vivo were very similar although the CCT at 2 months appeared substantially lower for RGX (23% lower than controls) than for UVX (11% lower than controls). The consistently lower in vivo CCT than in controls suggests that CXL may increase corneal collagen packing in the cross-linked region either due to crosslinking or remodeling. However, the thinner cornea for RGX than UVX was unexpected because RB penetrates, and crosslinks after green light exposure, only approximately the outermost 100 μm of stroma,[11] whereas UVX is estimated to crosslink the outermost two-thirds of a rabbit cornea (179–188 μm, Table 1).[8] The cornea deformation parameters report on the entire cornea, not just the cross-linked region. However, the material properties derived from finite element modeling reported here are for the cross-linked region. Similar to reported in our earlier publication for ex vivo treatment CXL treatments,[6] in vivo RGX stiffened the cornea to a greater degree than UVX in the cross-linked region (E_{eq} in Table 2) by factors of 2 and 1.46 at 1 and 2 months suggesting a greater density of crosslinks produced by RGX.

In summary, corneal biomechanical properties determined after ex vivo CXL are similar to but greater in magnitude than those obtained by in vivo CXL and consequently may not provide entirely accurate information about the responses to in vivo CXL. In vivo CXL followed over time demonstrates that corneal stiffness increases as a function of time after both RGX and UVX.

Acknowledgments

Supported by the European Research Council under the European Union's Seventh Framework Program ERC Advanced Grant agreement no. 294099; Comunidad de Madrid and EU Marie Curie

COFUND program (FP7/2007-2013/REA 291820); and the Spanish Government Grant FIS2014-56643-R.

Disclosure: **N. Bekesi**, None; **P. Gallego-Muñoz**, None; **L. Ibarés-Frías**, None; **P. Perez-Merino**, None; **M.C. Martinez-Garcia**, None; **I.E. Kochevar**, None; **S. Marcos**, None

References

1. Salgado JP, Khoramnia R, Lohmann CP, Winkler von Mohrenfels C. Corneal collagen crosslinking in post-LASIK keratectasia. *Br J Ophthalmol*. 2011;95:493–497.
2. Mita M, Waring GO IV, Tomita M. High-irradiance accelerated collagen crosslinking for the treatment of keratoconus: six-month results. *J Cataract Refract Surg*. 2014;40:1032–1040.
3. Mrochen M. Current status of accelerated corneal crosslinking. *Indian J Ophthalmol*. 2013;61:428–429.
4. Hafezi F, Mrochen M, Iseli HP, Seiler T. Collagen crosslinking with ultraviolet-A and hypoosmolar riboflavin solution in thin corneas. *J Cataract Refract Surg*. 2009;35:621–624.
5. Raiskup F, Spoerl E. Corneal cross-linking with hypo-osmolar riboflavin solution in thin keratoconic corneas. *Am J Ophthalmol*. 2011;152:28–32.e21.
6. Bekesi N, Kochevar IE, Marcos S. Corneal biomechanical response following collagen cross-linking with rose bengal-green light and riboflavin-UVA. *Invest Ophthalmol Vis Sci*. 2016;57:992–1001.
7. Dorronsoro C, Pascual D, Perez-Merino P, Kling S, Marcos S. Dynamic OCT measurement of corneal deformation by an air puff in normal and cross-linked corneas. *Biomed Opt Express*. 2012;3:473–487.
8. Gallhoefer NS, Spiess BM, Guscetti F, et al. Penetration depth of corneal cross-linking with riboflavin and UV-A (CXL) in horses and rabbits. *Vet Ophthalmol*. 2015;19:275–284.
9. Kling S, Ginis H, Marcos S. Corneal biomechanical properties from two-dimensional corneal flap extensiometry: application to UV-riboflavin cross-linking. *Invest Ophthalmol Vis Sci*. 2012;53:5010–5015.
10. Kohlhaas M, Spoerl E, Schilde T, Unger G, Wittig C, Pillunat LE. Biomechanical evidence of the distribution of cross-links in corneas treated with riboflavin and ultraviolet A light. *J Cataract Refract Surg*. 2006;32:279–283.
11. Cherfan D, Verter EE, Melki S, et al. Collagen cross-linking using rose bengal and green light to increase corneal stiffness. *Invest Ophthalmol Vis Sci*. 2013;54:3426–3433.
12. Zhu H, Alt C, Webb RH, Melki S, Kochevar IE. Corneal crosslinking with rose bengal and green light: efficacy and safety evaluation. *Cornea*. 2016;35:1234–1241.
13. Verter EE, Gisel TE, Yang P, Johnson AJ, Redmond RW, Kochevar IE. Light-initiated bonding of amniotic membrane to cornea. *Invest Ophthalmol Vis Sci*. 2011;52:9470–9477.
14. Yang P, Yao M, DeMartelaere SL, Redmond RW, Kochevar IE. Light-activated sutureless closure of wounds in thin skin. *Lasers Surg Med*. 2012;44:163–167.
15. Marcos S, Alejandre N, Lamela J, Dorronsoro C, Kochevar IE. Toward new engagement paradigms for intraocular lenses: light-initiated bonding of capsular bag to lens materials. *Invest Ophthalmol Vis Sci*. 2015;56:4249–4256.
16. Scarcelli G, Kling S, Quijano E, Pineda R, Marcos S, Yun SH. Brillouin microscopy of collagen crosslinking: noncontact depth-dependent analysis of corneal elastic modulus. *Invest Ophthalmol Vis Sci*. 2013;54:1418–1425.
17. Dias J, Diakonis VF, Lorenzo M, et al. Corneal stromal elasticity and viscoelasticity assessed by atomic force microscopy after different cross linking protocols. *Exp Eye Res*. 2015;138:1–5.
18. Kling S, Remon L, Perez-Escudero A, Merayo-Lloves J, Marcos S. Corneal biomechanical changes after collagen cross-linking from porcine eye inflation experiments. *Invest Ophthalmol Vis Sci*. 2010;51:3961–3968.
19. Wollensak G, Iomdina E. Biomechanical and histological changes after corneal crosslinking with and without epithelial debridement. *J Cataract Refract Surg*. 2009;35:540–546.
20. Medeiros FA, Weinreb RN. Evaluation of the influence of corneal biomechanical properties on intraocular pressure measurements using the ocular response analyzer. *J Glaucoma*. 2006;15:364–370.
21. Tian L, Huang YF, Wang LQ, et al. Corneal biomechanical assessment using corneal visualization scheimpflug technology in keratoconic and normal eyes. *J Ophthalmol*. 2014;2014:147516.
22. Bekesi N, Dorronsoro C, de la Hoz A, Marcos S. Material properties from air puff corneal deformation by numerical simulations on model corneas. *PLoS One*. 2016;11:e0165669.
23. Greenstein SA, Fry KL, Hersh PS. In vivo biomechanical changes after corneal collagen cross-linking for keratoconus and corneal ectasia: 1-year analysis of a randomized, controlled, clinical trial. *Cornea*. 2012;31:2–25.
24. De Bernardo M, Capasso L, Lanza M, et al. Long-term results of corneal collagen crosslinking for progressive keratoconus. *J Optom*. 2015;8:180–186.
25. Kling S, Akca IB, Chang EW, et al. Numerical model of optical coherence tomographic vibrography imaging to estimate corneal biomechanical properties. *J R Soc Interface*. 2014;11:20140920.
26. Kling S, Bekesi N, Dorronsoro C, Pascual D, Marcos S. Corneal viscoelastic properties from finite-element analysis of in vivo air-puff deformation. *PLoS One*. 2014;9:e104904.
27. Kling S, Marcos S. Effect of hydration state and storage media on corneal biomechanical response from in vitro inflation tests. *J Refract Surg*. 2013;29:490–497.
28. Boote C, Dooley EP, Gardner SJ, et al. Quantification of collagen ultrastructure after penetrating keratoplasty - implications for corneal biomechanics. *PLoS One*. 2013;8:e68166.
29. Sorkin N, Varssano D. Corneal collagen crosslinking: a systematic review. *Ophthalmologica*. 2014;232:10–27.
30. ANSYS, Inc. *Workbench Version 15.0 User Manual*. Canonsburg, PA: ANSYS, Inc.; 2013.
31. Hammer A, Kling S, Boldi MO, et al. Establishing corneal cross-linking with riboflavin and UV-A in the mouse cornea in vivo: biomechanical analysis. *Invest Ophthalmol Vis Sci*. 2015;56:6581–6590.
32. Elsheikh A, Geraghty B, Rama P, Campanelli M, Meek KM. Characterization of age-related variation in corneal biomechanical properties. *J R Soc Interface*. 2010;7:1475–1485.
33. Chunyu T, Xiujun P, Zhengjun F, Xia Z, Feihu Z. Corneal collagen cross-linking in keratoconus: a systematic review and meta-analysis. *Sci Rep*. 2014;4:5652.
34. Goldich Y, Marcovich AL, Barkana Y, et al. Clinical and corneal biomechanical changes after collagen cross-linking with riboflavin and UV irradiation in patients with progressive keratoconus: results after 2 years of follow-up. *Cornea*. 2012;31:609–614.